Journal of Molecular Catalysis A: Chemical 301 (2009) 159–165

Contents lists available at ScienceDirect

Journal of Molecular Catalysis A: Chemical

journal homepage: www.elsevier.com/locate/molcata

Ethane dehydrogenation over pore-expanded mesoporous silica-supported chromium oxide: 2. Catalytic properties and nature of active sites

T.V. Malleswara Rao, El Mamoune Zahidi[1], Abdelhamid Sayari*

Department of Chemistry, University of Ottawa, Ottawa, ON, Canada K1N 6N5

ARTICLE INFO

Article history:
Received 5 September 2008
Received in revised form
27 November 2008
Accepted 27 December 2008
Available online 9 January 2009

Keywords:
Ethane dehydrogenation
Chromium oxide
Pore-expanded MCM-41
XPS

ABSTRACT

Pore-expanded mesoporous MCM-41 silica-supported chromium oxide catalysts with different chromia loadings were synthesized using three different methods. The catalysts were thoroughly characterized and used for ethane dehydrogenation (DH). Reaction studies revealed that the ethane conversion and coke formation on the catalyst depend on the chromia loading and the catalyst preparation method. All catalysts were highly selective toward ethylene. However, among the three catalysts containing 5 wt% chromia, the 5 wt% Cr/PE-MCM-41 catalyst exhibited the best performance with an ethane conversion of 23% and ~99% ethylene selectivity at 650 °C (C_2H_6/N_2 = 0.176, total contact time = 0.0032 g min/mL). The chromia catalysts prepared using as-synthesized pore-expanded mesoporous silica (Cr/PE-MCM-41) also exhibited the highest stability. XPS analysis revealed the presence of three different chromium, namely Cr(II), Cr(III) and Cr(VI), whose overall surface concentration as well as relative content varied with the reaction time-on-stream (TOS). Furthermore, the nature and relative amounts of surface chromium species were monitored by *in situ* XPS measurements as a function of TOS. Correlation of the XPS findings with ethane DH data showed clearly that the Cr(III) species are the main active sites.

1. Introduction

Due to its equilibrium limitations and endothermic nature, the ethane dehydrogenation (DH) process is favored at relatively low pressures and high temperatures. However, such conditions usually lead to decreased ethylene selectivity due to overcracking phenomenon and to severe deactivation of the catalyst because of coke formation [1–3]. Thus, developing novel catalysts, which are highly selective and capable of withstanding large coke build-up while maintaining high catalytic activity for prolonged times, would be an important achievement.

Despite the importance of ethane DH, only few studies dealt with this reaction over catalysts such as rhenium [4], gallium oxide [5], and chromium oxide [1,6–11]. Rovik et al. [4] investigated 2.8 wt% Re catalyst supported on mesoporous MFI zeolite (Si/Al > 500) for ethane DH at 550 °C and found it to be relatively stable at low conversions (2–6%). However, the performance of the catalysts was not investigated at higher temperatures (>550 °C) to achieve higher conversions. Nakagawa et al. [5] studied ethane DH over several metal oxide catalysts for only 30 min time-on-stream. They found Ga_2O_3 to be the best catalyst compared to other metal oxides but the stability or life time of the catalyst was not reported. Supported chromium oxide catalysts were also found to be effective for DH of ethane [6–11] and most of these studies focused mainly on elucidating the role of chromium active sites. However, the nature of chromium active sites is still being debated as both Cr(II) [6,7] and Cr(III) [11–14] species were reported to be the active sites for light alkane DH. Furthermore, there is very little information available on the stability and regenerability of supported chromia catalysts for ethane DH.

Pore-expanded mesoporous MCM-41 silica exhibits a unique combination of high surface area (>1000 m^2/g), large pore sizes (up to 25 nm) and high pore volume (up to 3.6 cm^3/g) [15–17]. Over the past few years, several applications for pore-expanded mesoporous silica in adsorption [18–22] and catalysis [23,24] were reported. The objective of the current investigation is the development of stable, highly selective and active ethane DH catalysts based on chromium oxide supported on pore-expanded mesoporous silica. Another major thrust of this work is the use of quasi *in situ* X-ray photoelectron spectroscopy (XPS) to monitor the catalysts surface during ethane DH. To the best of our knowledge, there are no other studies on quasi *in situ* XPS investigation of supported chromia catalysts at different stages of ethane DH. Correlation of XPS findings and catalytic activity provided strong evidence that Cr(III) is the active site for ethane DH. Notice that the synthesis and detailed characterization of three series of chromia-containing catalysts have been reported in a companion paper [25].

* Corresponding author. Tel.: +1 613 562 5483; fax: +1 613 562 5170.
E-mail address: abdel.sayari@uottawa.ca (A. Sayari).
[1] Current address: Chouaïb Doukkali University, Faculty of Sciences, Department of Chemistry, El Jadida, Morocco.

1381-1169/$ – see front matter © 2009 Elsevier B.V. All rights reserved.
doi:10.1016/j.molcata.2008.12.027

2. Experimental

2.1. Catalysts preparation

As stated earlier, all the chromia-based catalysts were described elsewhere [25]. The pore-expanded MCM-41 silica was prepared in two stages, namely the synthesis of conventional MCM-41 silica in the presence of cetyltrimethylammonium bromide (CTAB) followed by the hydrothermal pore-expansion process in the presence of dimethyldecylamine (DMDA) as a swelling agent.

The chromia-based catalysts were prepared using the three following methods.

- *Method I*: The as-synthesized PE-MCM-41 silica, i.e., filled with CTA cations and DMDA was used as support. The chromium was loaded through complexation by the occluded DMDA followed by calcination in air at 700 °C. The obtained catalysts are denoted as *x*Cr/PE-MCM-41, where *x* is the wt% loading corresponding to Cr_2O_3.
- *Method II*: Selective extraction of DMDA in as-synthesized PE-MCM-41 silica afforded PE-MCM-41E, which was used as catalyst support. Supported chromia catalysts were prepared by the incipient wetness impregnation technique followed by calcination in air at 700 °C. The catalysts thus obtained are referred to as *x*Cr/PE-MCM-41E, where *x* is the wt% loading corresponding to Cr_2O_3.
- *Method III*: The as-synthesized PE-MCM-41 silica was calcined at 700 °C and used as support. Deposition of chromium was achieved by the incipient wetness impregnation technique as described in Method II using the calcined support. Only one sample, 5Cr/PE-MCM-41C with ~5 wt% chromia loading was prepared.

2.2. Catalysts characterization

Detailed characterization of the catalysts using nitrogen adsorption, X-ray diffraction, temperature-programmed reduction was reported elsewhere [25]. UV–vis diffuse reflectance spectroscopy measurements were obtained using a Varian Cary 300 spectrometer.

As reported earlier [25], X-Ray Photoelectron Spectroscopy (XPS) measurements on supported chromium oxide catalysts were performed on a Kratos Axis Ultra DLD spectrometer using a focused monochromatized Al Kα radiation (1486.6 eV). Charging effects of the sample were minimized by employing a low energy electron gun. High resolution XPS spectra were obtained at 20 eV pass energy in a short period of time (~12 min) in order to avoid or minimize the reduction of surface chromium species induced by X-rays [26–28]. The binding energies were calibrated using the peak of adventitious carbon (C 1s) at 284.6 eV [28]. Quantitative calculations of the surface atomic concentrations and the composition of different chemical states of surface chromium were obtained by peak fitting of XPS spectra using Vision 2.0 processing software, provided by Kratos Analytical Ltd., UK.

The quasi *in situ* XPS analysis over the supported chromia catalyst during activation and ethane dehydrogenation was carried out using the same instrument, which was also equipped with an integrated high pressure, high temperature catalytic reaction cell. This cell was capable of operating at temperatures up to 900 °C and pressures up to 10 atm. The ethane DH reaction was carried out in this cell at conditions similar to those used for the conventional fixed-bed reactor studies to establish a structure-reactivity relationship. The quasi *in situ* XPS spectra were obtained using the following procedure. The sample was pressed into a pellet corresponding to the dimensions of a quartz sample holder especially designed for the catalytic reaction cell. XPS spectra were obtained for this fresh catalyst using the same procedure as described above for *ex situ* analysis. The sample was then transferred internally (without exposing to the atmosphere) to the reaction cell using sample transfer rods. The sample was initially heated *in situ* in flowing N_2 (50 mL/min) to 650 °C and 1 atm pressure, and subsequently pretreated in high purity air at 650 °C for 30 min, followed by N_2 purging for 30 min. After cooling the sample to room temperature (RT), it was transferred to the XPS analysis chamber, without exposure to air. After XPS measurements, the sample was again moved to the reaction cell, where it was heated to 650 °C in flowing N_2. The ethane DH reaction was then performed for 15 min time-on-stream (TOS) at 650 °C and 1 atm pressure using a 50% C_2H_6/N_2 reaction feed with a total flow rate of 50 mL/min. The XPS spectra of the sample after reaction was acquired as described above, i.e., cooling the sample after reaction in N_2 to RT and further transfer to the XPS chamber. Similar XPS measurements after reaction at different TOS values were collected using the procedure described above. The reaction time was reported in terms of cumulative TOS values. For instance, the reaction time would be 1 h if the reaction was carried out for 15 min followed by XPS analysis and then for 45 min. The XPS findings were used to identify and quantify the different chemical states of surface chromium species, and to elucidate the nature of the active sites in ethane DH reaction.

2.3. Ethane DH reaction studies

The prepared catalysts were tested for ethane DH at atmospheric pressure in a vertical down-flow fixed-bed U-tube quartz reactor mounted in a tubular furnace. Typically, 0.16 g of catalyst was employed. The temperature of the catalyst bed was measured by a thermocouple located in a quartz well placed in the catalyst bed, and was controlled by a PID temperature controller. The flow rates of reactant and pretreatment gases were adjusted through separate MKS mass flow controllers. Prior to the reaction studies the catalyst sample was heated in flowing N_2 (50 mL/min) to 700 °C, then in air (50 mL/min) at the same temperature for 30 min, followed by N_2 purging for 15 min. After cooling the catalyst to 600 °C in N_2, the reaction feed containing ethane (C_2H_6) and nitrogen (N_2) was introduced into the reactor at a specific molar ratio with a constant total flow rate of 50 mL/min. The effluent gases from the reactor were directed for online analysis to a gas chromatograph (Agilent 6890N) through a heated transfer line. The reactant and products formed (C_2H_6, C_2H_4 and CH_4) were separated using a GS-GasPro PLOT capillary column (60 m × 0.32 mm ID) and analyzed using a flame ionization detector. The temperature of the catalyst was varied between 600 and 650 °C. The mole fraction of C_2H_6 ($x_{C_2H_6}$) in the feed was varied between 0.15 and 0.5 in order to study the effect of dilution of ethane on the catalytic performance. Initially, the reaction was carried out at 600 °C and the effluent was analyzed at 7 min of TOS, and subsequent measurements were taken every ~10 min on stream up to 1 h. After that, the catalyst was purged at the same temperature with N_2 for 30 min and the flow was switched to air (50 mL/min) for 40 min to regenerate the catalyst, followed by N_2 purging for 30 min. The temperature was then changed to 625 °C and the reaction data were collected as described above. Data at other temperatures were obtained using the same procedure. Based on the inlet and outlet concentrations, the conversion, selectivity and yields were calculated. These calculations were based on the moles of products formed, but not on the basis of ethane consumption as there was a loss of some carbon due to coke deposition on the catalyst during ethane DH.

Blank experiments were also conducted in the absence of catalyst at different temperatures ranging from 600 to 700 °C to investigate the contribution of thermal dehydrogenation of ethane, if any. Based on these runs, the temperature range of 600–650 °C was found to be appropriate for catalytic studies.

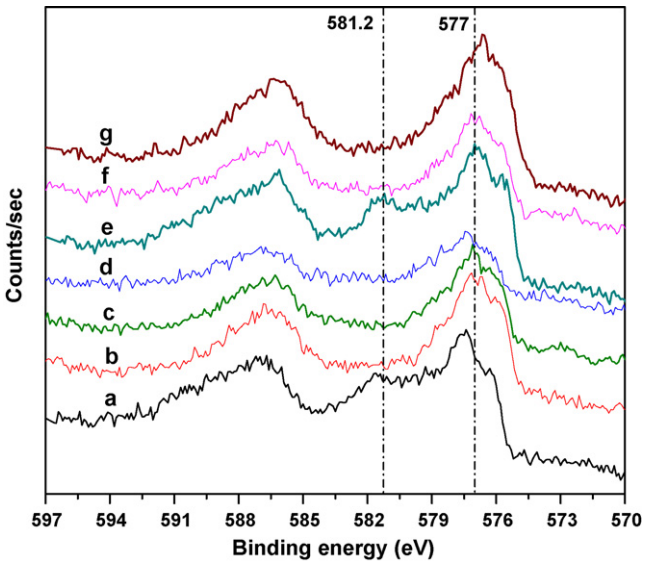

Fig. 1. Quasi *in situ* XPS Cr 2p region spectra at 650 °C; $x_{C_2H_6} = 0.5$; total flow rate = 50 mL/min: (a) pretreated in air for 30 min; (b) after 15 min time-on-stream (TOS); (c) after 1 h TOS; (d) after 3 h TOS; (e) regenerated in air for 2 h; (f) after 2nd cycle reaction at TOS of 1 h; (g) pre-reduced in 50% H_2/N_2 for 1.5 h.

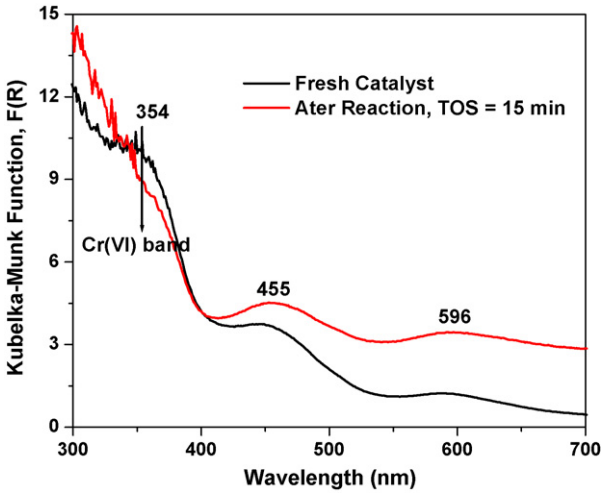

Fig. 2. UV–vis DRS spectra of the 5Cr/PE-MCM-41 catalyst before and after reaction.

The coke deposited on the catalyst during ethane DH was evaluated by thermogravimetic analysis (TGA) using a TA Instruments TGA Q500 analyzer. To examine the catalyst stability, the reaction was conducted at the highest temperature considered (650 °C) for 24 h. The spent catalysts were regenerated overnight in air and further tested for ethane DH activity.

3. Results and discussion

3.1. XPS

All Cr 2p spectra were comprised of two peaks centered at ~577 and ~586.5 eV, corresponding to Cr $2p_{3/2}$ and Cr $2p_{1/2}$ photoelectrons, respectively [25]. The Cr $2p_{3/2}$ band was deconvoluted into three components with binding energy values of ~576, ~577 and ~581 eV, corresponding to Cr(II), Cr(III) and Cr(VI) species, respectively [27,29]. The surface concentration of chromium as well as the relative amount of chromium species in as-synthesized catalysts, i.e., calcined at 700 °C and exposed to ambient air were reported earlier [25]. The 5Cr/PE-MCM-41C contained comparable amounts of all three chromium species, whereas the other two series of catalysts *x*Cr/PE-MCM-41 and *x*Cr/PE-MCM-41E contained very little surface Cr(II) and significant amounts of Cr(III) and Cr(VI).

The quasi *in situ* XPS studies of ethane DH were carried out using a 50% C_2H_6/N_2 mixture (50 mL/min) at 650 °C on the 5Cr/PE-MCM-41 catalyst that was chosen based on the best catalytic performance in the conventional fixed bed reactor studies, which are discussed later. The XPS Cr 2p spectra of the 5Cr/PE-MCM-41 catalyst under different conditions are depicted in Fig. 1. The precalcined fresh catalyst (spectrum a in Fig. 1) showed clearly two Cr $2p_{3/2}$ bands corresponding to Cr(III) (577.4 eV) and Cr(VI) (581.2 eV) species and a small shoulder at 576.2 eV, associated with Cr(II) species [27,29]. Quantification results of the spectra by deconvolution are presented in Table 1. The predominant chromium species present on the precalcined catalyst were Cr(III) and Cr(VI) species with a minor contribution from Cr(II) (~4%). It is clear from Fig. 1 (spectrum b) and Table 1 that after 15 min of ethane DH reaction, the percentage of Cr(VI) species decreased from ~41 to 15%, while the Cr(III) concentration increased from 55 to 80%, indicating that the majority of Cr(VI) species were reduced to Cr(III) during the initial stage of reaction. Furthermore, the XPS data showed that the most predominant species observed at all TOS values was Cr(III) (~80–90%) with minor contributions from Cr(II) and Cr(VI) species. However, the overall surface chromium concentration decreased continuously with increasing TOS because of the coke formation on the catalyst surface during ethane DH. At higher TOS values, the coke deposited on the catalyst made it difficult to determine the exact composition of different chromium species present. After regenerating the catalyst in air at 650 °C, the highly oxidized Cr(VI) species was restored as evidenced by the reappearance of a XPS signal at 581.2 eV (spectrum e) and the calculated surface composition (Table 1).

The rapid reduction of Cr(VI) species upon exposure to the reaction conditions was also confirmed by the *ex situ* UV–vis diffuse reflectance spectroscopy results shown in Fig. 2. The UV–vis spectrum of the fresh 5Cr/PE-MCM-41 catalyst revealed absorption bands at ~354 nm due to the presence of Cr(VI) species and at ~455 and ~596 nm due to Cr(III) species [30,31]. The UV–vis spectrum of the catalyst after reaction (TOS = 15 min) showed that the band due to Cr(VI) (~354 nm) species nearly disappeared indicating the rapid reduction of Cr(VI) species during the initial stage of reaction, whereas the bands due to Cr(III) remained with a slight shift towards higher wavenumbers. The fast reduction of Cr(VI) to Cr(III) species during propane DH over supported chromia was also

Table 1
XPS (quasi *in situ*) results for the 5Cr/PE-MCM-41catalyst.

Catalyst treatment	Cr $2p_{3/2}$ Binding energy (eV)			Cr, atomic concentration (%)	Percentage of different Cr species (%)		
	Cr(VI)	Cr(III)	Cr(II)		Cr(VI)	Cr(III)	Cr(II)
Pretreated in air	581.0	577.4	576.2	2.70	41.3	55.3	4.4
After TOS = 15 min	580.9	577.2	576.1	2.18	15.1	81.5	4.4
After TOS = 1 h	581.0	577.0	576.0	1.97	8.0	88.9	3.1
After TOS = 3 h	581.1	577.3	576.2	1.67	8.0	99.8	2.2
Regenerated in air	580.9	577.1	575.9	2.72	40.5	57.4	2.2
Reaction 2nd cycle, after TOS = 1 h	580.8	577.2	576.3	2.15	16.9	78.7	4.4

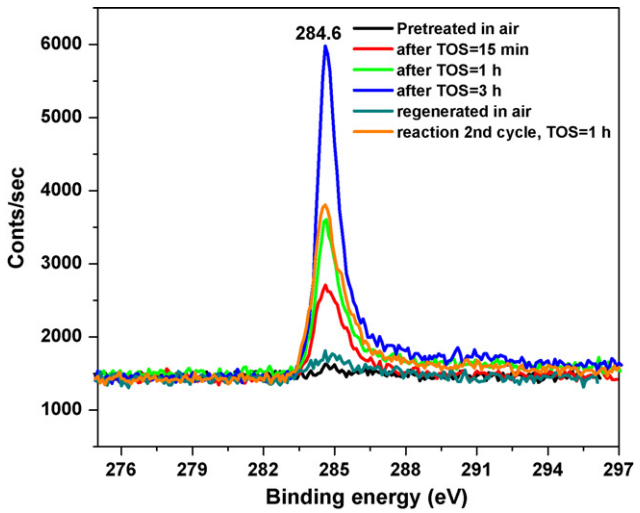

Fig. 3. Quasi *in situ* XPS C 1s region spectra under different conditions.

observed *in-situ* UV–vis spectroscopy [32–35]. In fact, the Cr(VI) reduction to Cr(III) occurred in a propane/N_2 stream at much lower temperature than the current reaction temperature [32]. Furthermore, as seen in Fig. 2, an increase in absorbance was observed in the UV–vis spectrum of the spent catalyst. Similar findings for propane DH over supported chromia catalysts were attributed to the coke formed on the catalyst surface [32].

To understand the behavior of coke deposition on the catalyst surface, the C 1s spectra (centered at 284.6 eV) were recorded under different conditions (Fig. 3). As shown, the intensity of the C 1s peak for the precalcined catalyst was very small, indicating the occurrence of only a trace amount of carbon before reaction. The carbon deposition on the catalyst surface increased with TOS as evidenced by the increasing intensity of the C 1s peak. Furthermore, the carbon deposition decreased to trace amounts upon regenerating the catalyst in air at 650 °C. After running a 2nd cycle of ethane DH reaction for 1 h using the regenerated catalyst, the C 1s peak intensity increased again and almost matched the peak observed in the 1st cycle of reaction for 1 h. This suggests that the behavior of coke formation during ethane DH is similar at a particular TOS value even after few cycles of reaction, indicating the high stability of the catalyst.

3.2. Ethane dehydrogenation

The ethane DH reaction was first carried out in the absence of a catalyst for 30 min at different temperatures ranging from 600 to 700 °C using an equimolar C_2H_6/N_2 mixture to examine the contribution of thermal dehydrogenation. As shown in Table 2, the only products observed were ethylene (C_2H_4) and a trace amount of methane (CH_4). It is clear from Table 2 that indeed there was a contribution from ethane thermal dehydrogenation starting at 650 °C and becomes very significant at temperatures above 675 °C. The chromium-free PE-MCM-41C silica support (0.16 g) was also tested for ethane DH under the same conditions as mentioned above and the data are given in Table 2. The conversions obtained were similar to those for thermal dehydrogenation, suggesting that the PE-MCM-41C support is inactive for ethane DH.

Table 2
Ethane thermal dehydrogenation data; reaction conditions: $x_{C_2H_6} = 0.5$, TOS = 30 min.

Sample	Temperature (°C)	Ethane conversion (%)	Selectivity (%)	
			C_2H_4	CH_4
Empty reactor	625	0	–	–
	650	1.5	99.2	0.8
	675	4.3	98.5	1.5
	700	10.2	97.4	2.6
PE-MCM-41C	625	0	–	–
	650	1.5	99.3	0.7
	675	4.5	98.3	1.7
	700	10.3	97.2	2.8

Table 3
Ethane dehydrogenation over bulk and supported chromium oxide catalysts: weight of the catalyst = 0.16 g; total flow rate = 50 mL/min; mole fraction of C_2H_6, $x_{C_2H_6}$ = 0.5.

Catalyst	Temperature (°C)	Ethane conversion (%)		Selectivity (%)	
		TOS = 7 min	TOS = 60 min	C_2H_4	CH_4
2Cr/PE-MCM-41	600	5.3	5.2	100	0
	625	9.5	8.8	99.2	0.8
	650	15.6	14.5	98.9	1.0
5Cr/PE-MCM-41	600	7.7	6.9	99.4	0.6
	625	11.5	10.5	99.1	0.9
	650	17.4	15.7	98.8	1.2
2Cr/PE-MCM-41E	600	6.7	6.0	100	0
	625	10.4	8.7	99.4	0.6
	650	16.1	13.3	99.0	1.0
5Cr/PE-MCM-41E	600	9.0	7.4	99.3	0.7
	625	12.5	10.5	99.0	1.0
	650	18.7	14.8	98.2	1.8
7Cr/PE-MCM-41E	600	6.4	4.3	99.6	0.4
	625	8.4	6.5	99.2	0.8
	650	13.4	9.6	98.8	1.2
5Cr/PE-MCM-41C	600	6.4	4.0	100	0
	625	9.1	6.1	99.5	0.5
	650	12.3	8.2	99.3	0.7
Bulk Cr_2O_3	600	1.2	0.8	100	0
	625	1.7	1.0	100	0
	650	2.8	2.0	100	0

Based on these preliminary observations, the ethane DH studies were performed over bulk and supported chromium oxide catalysts at an iso-contact time of 0.0032 g min/mL in the temperature range of 600–650 °C and at $x_{C_2H_6}$ of 0.5. Similar to the thermal dehydrogenation, the products observed in the catalytic ethane DH were C_2H_4 and trace amounts of CH_4. The ethane conversion and selectivity were measured for all catalysts at different TOS values and the results at 7 and 60 min are summarized in Table 3. The selectivities were calculated based on the products detected without taking into account the coke deposited on the catalyst during the reaction. It can be seen from Table 3 that for all the catalysts, the ethane conversion at a particular TOS value increased with increasing temperature and was lower than the equilibrium conversion (given in Table 4) at that particular reaction conditions. The equilibrium conversions for the ethane DH reaction were calculated based on the equilibrium constants obtained at different temperatures using standard Gibbs free energy change and heat of reaction by considering the temperature effect on the heat of reaction without any assumption of constant heat capacity [36,37]. In order to

Table 4
Equilibrium conversion for ethane DH at different reaction conditions.

Temperature, T (°C)	Equilibrium constant, K	Mole fraction of C_2H_6, $x_{C_2H_6}$	Equilibrium conversion, X_e (%)
600	0.0285	0.5	22.18
625	0.0494	0.5	28.43
650	0.0834	0.5	35.57
650	0.0834	0.3	42.45
650	0.0834	0.15	53.06

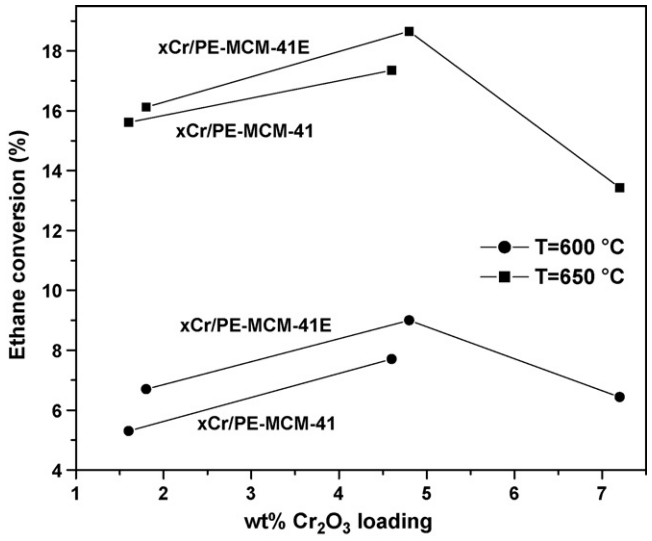

Fig. 4. Effect of chromia loading on the initial ethane conversion; TOS = 7 min and $x_{C_2H_6} = 0.5$.

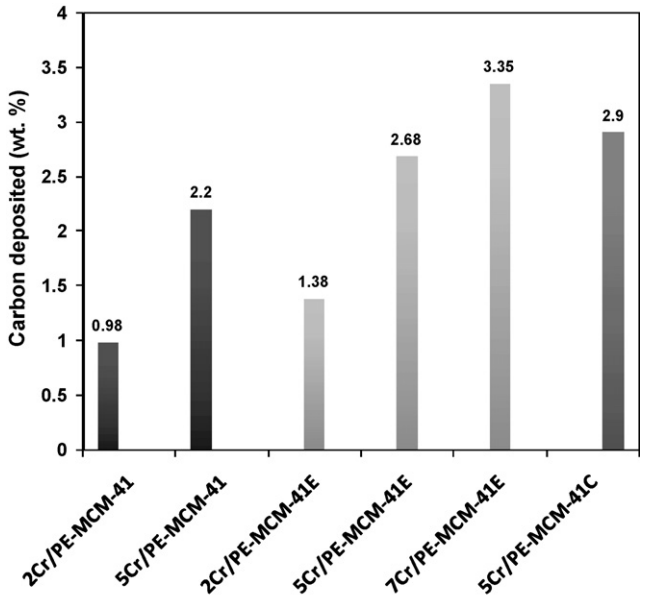

Fig. 5. Coke deposited on the catalysts during ethane DH reaction; temperature = 650 °C, TOS = 1 h and $x_{C_2H_6} = 0.5$.

perform the above analysis, thermodynamic properties required for each compound were taken from published data [37]. Table 4 shows that the equilibrium constant (K) and equilibrium conversion (X_e) values increase with increasing temperature, consistent with the endothermic nature of ethane DH. The equilibrium conversion, however, also depends on the feed composition and it increases with an increase in dilution of ethane in the feed. Furthermore, as the TOS increased from 7 to 60 min, the ethane conversion decreased for all the catalysts. However, it appears from Table 3 that the extent of decrease in ethane conversion depends on the temperature and the catalyst used. To further investigate this behavior, catalyst stability experiments were carried out and are discussed later.

All the supported chromium oxide catalysts were found to be highly selective towards ethylene formation. The C_2H_4 selectivity was always around 99% regardless of the operating conditions and the catalysts used. The effect of chromia loading on the initial (TOS = 7 min) ethane conversion for *x*Cr/PE-MCM-41 and *x*Cr/PE-MCM-41E catalysts at 600 and 650 °C is presented in Fig. 4. It can be observed that at a particular temperature, the ethane conversion initially increased with increasing chromia loading for both series of catalysts. For example, the ethane conversion for *x*Cr/PE-MCM-41E catalysts increased with increasing chromia loading up to 5 wt% and decreased for higher loading sample, most likely because of the presence of a large amount of Cr_2O_3 crystallites as confirmed by XRD. Similar trends were also observed at other TOS values. Furthermore, the *x*Cr/PE-MCM-41E samples were slightly more active than the *x*Cr/PE-MCM-41 samples during the initial stage of reaction.

To quantify the amount of coke deposited on the catalysts after 1 h of reaction at 650 °C, the spent catalysts were subjected to thermogravimetic analysis (TGA) by heating the sample to 800 °C in N_2 and from 800 to 1000 °C in air. The results are shown in Fig. 5. As seen, the coke formed on the catalyst surface (expressed in wt%) increased with increasing chromia loading and at a particular chromia loading it followed the order: 5Cr/PE-MCM-41 < 5Cr/PE-MCM-41E < 5Cr/PE-MCM-41C. The amount of coke determined by TGA experiments was consistent (±10% deviation) with the loss of carbon obtained from the carbon balance calculations based on the feed and the effluent gas concentrations. Thus, it appears that the coke formation is lower on the catalysts prepared by Method I compared to the other catalysts.

The effect of ethane DH reaction on the pore structure characteristics was also investigated for 5Cr/PE-MCM-41 and 5Cr/PE-MCM-41E catalysts after 1 h reaction at 650 °C and $x_{C_2H_6}$ of 0.5. The corresponding pore size distributions are presented in Fig. 6. Comparison of the pore size distributions (PSDs) of the catalysts before and after reaction indicates that the average pore sizes of the catalysts remained unchanged after 1 h of reaction. It was also observed that the surface area of the spent catalysts decreased slightly from 1065 to 986 m^2/g for 5Cr/PE-MCM-41 and from 925 to 825 m^2/g for the 5Cr/PE-MCM-41E catalyst due to the coke formed on the catalysts. The pore volumes also decreased slightly after 1 h of reaction.

The effect of dilution on ethane conversion was studied at 650 °C for 1 h TOS by increasing the mole fraction of N_2 in the C_2H_6/N_2 reaction feed. Fig. 7 shows the variation of ethane conversion with the dilution of ethane in the feed for the ~5 wt% chromia containing samples prepared by different methods. The conversion increased with increasing dilution for all the catalysts. This trend is in line

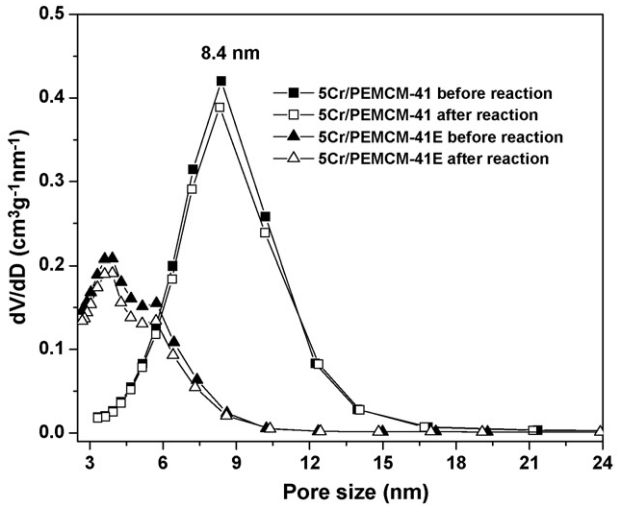

Fig. 6. Pore size distributions of the spent catalysts; temperature = 650 °C, TOS = 1 h and $x_{C_2H_6} = 0.5$.

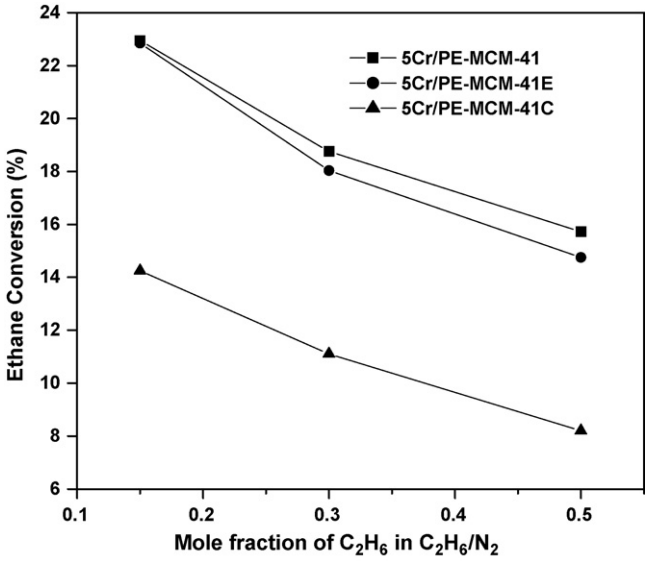

Fig. 7. Effect of dilution of ethane reactant feed on ethane conversion; temperature = 650 °C and TOS = 1 h.

with the equilibrium conversion trend, which also increases with increasing dilution of the feed at a particular reaction temperature (Table 4). Furthermore, the C_2H_4 selectivity was always around 99% at all dilutions of feed (data not shown).

In order to examine the stability and regenerability of the catalysts prepared by different methods, ethane DH was carried out over ~5 wt% chromia loaded samples for a prolonged time (~24 h) and the data are presented in Fig. 8. The C_2H_4 selectivity was found to be relatively constant (~98–99%) throughout the reaction. It can be seen from Fig. 8 that for the 5Cr/PE-MCM-41 and 5Cr/PE-MCM-41E catalysts, the ethane conversion decreases slowly as the TOS increases, while it decreases at a faster rate for 5Cr/PE-MCM-41C. Furthermore, the rate of decrease in ethane conversion was faster at the initial stage of reaction (up to 5 h) and slower at higher TOS values. This may be explained in terms of carbon balance calculations based on the inlet and outlet concentrations of the carbon compounds. Depending on the catalyst used, the carbon balance was found to be around 89–93% in the first 10 h of reaction and 94–97% at higher TOS values and the highest deviation (9–11%) was observed during the first hour of reaction. This suggests that the coke deposition was predominant in the early stages of the reaction, which is consistent with the slower deactivation observed at high TOS values. However, it appears from Fig. 8 that the catalyst stability and activity strongly depend on the catalyst preparation method. The ethane conversion during the initial stage of reaction follows the order: 5Cr/PE-MCM-41 ~ 5Cr/PE-MCM-41E ≫ 5Cr/PE-MCM-41C, while it changes to 5Cr/PE-MCM-41 > 5Cr/PE-MCM-41E ≫ 5Cr/PE-MCM-41C at higher TOS values. The lower activity of 5Cr/PE-MCM-41C compared to that for the other two catalysts may be attributed to a combination of factors including its low surface area, the collapsed pore structure observed by N_2 adsorption measurements and the lower chromia dispersion as inferred from XRD data. Among the three catalysts studied, the 5Cr/PE-MCM-41 catalysts was found be the most stable and active catalyst due to its open pore structure and large pores, which allows it to preserve its dehydrogenation activity for extended period of time. The TGA results also showed that *x*Cr/PE-MCM-41 catalysts generated less coke compared to the other catalysts (see Fig. 5). Furthermore, the regenerability of the catalysts was examined by treating the spent catalysts in air and further testing for ethane DH reaction for ~3 h. From Fig. 8, it is interesting to note that the activity of all catalysts was completely restored after regeneration.

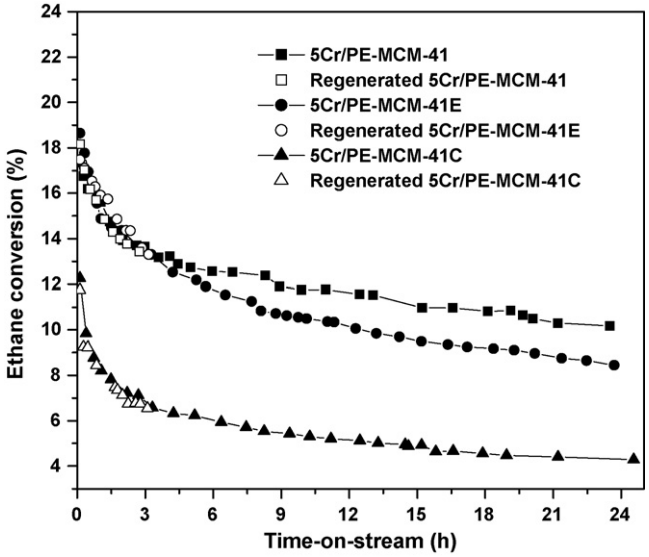

Fig. 8. Catalysts stability and regenerability at 650 °C; $x_{C_2H_6} = 0.5$.

3.3. Nature of the active sites

The quasi *in situ* XPS results of the 5Cr/PE-MCM-41 catalyst (Table 1) clearly showed that before reaction, the precalcined sample contained both Cr(VI) (41%) and Cr(III) (55%) as major species and a very small quantity of Cr(II) (4%) species. Furthermore, the *in situ* XPS measurements along with *ex situ* UV–vis data for the 5Cr/PE-MCM-41 catalyst revealed that under reaction conditions, the majority of Cr(VI) species reduced very fast to Cr(III). The spent catalyst contained mainly Cr(III) (80–90%) species and small amounts of Cr(VI) and Cr(II) species. Correlating these findings with the fixed-bed reaction data suggests that the Cr(III) species are the main active sites for the ethane DH reaction. The fact that in the early stages of reaction, the surface Cr(VI) species decreased much faster than the ethane conversion (63% in 15 min vs. 4%) indicates that Cr(VI) does not play any major role in ethane DH. Furthermore, because the surface concentration of Cr(II) species is always very small, it is unlikely that such species are involved in ethane DH. Interestingly, earlier studies involving *in situ* UV–vis/EPR [32,33], UV–vis/Raman [34,35] and FT-IR [13] spectroscopy revealed that the active sites in supported chromium oxide catalysts during propane DH are Cr(III) species. Based on on-line FT-IR analysis and UV–vis data, Hakuli et al. [38] attributed the iso-butane dehydrogenation activity of chromia/silica catalysts to redox Cr in 3+ and 2+ oxidation states and to part of non-redox Cr(III) species. Furthermore, based on *in situ* UV–vis diffuse reflectance spectroscopy data, Weckhuysen et al. [12] concluded that Cr(III) and Cr(II) are the active sites for n-butane DH, with Cr(III) being much more active than Cr(II) species. Thus, it appears that there is some consensus in the literature supporting the observation that Cr(III) species are the main active sites for light alkane DH.

To lend further support to the contention that Cr(III) species are the main active sites, the intrinsic activity of the catalyst (activity per surface Cr atom per second) or turnover frequency (TOF) was evaluated for the best catalyst, i.e., 5Cr/PE-MCM-41, combining *in situ* XPS data and the reaction rate as measured in fixed-bed catalytic studies. The TOF values were evaluated based on the total surface Cr concentration and also by assuming, one at a time, that Cr(II), Cr(III) and Cr(VI) species are the only active sites. It is important to take into account the variation of surface Cr concentration with TOS in TOF calculations because not only the overall surface

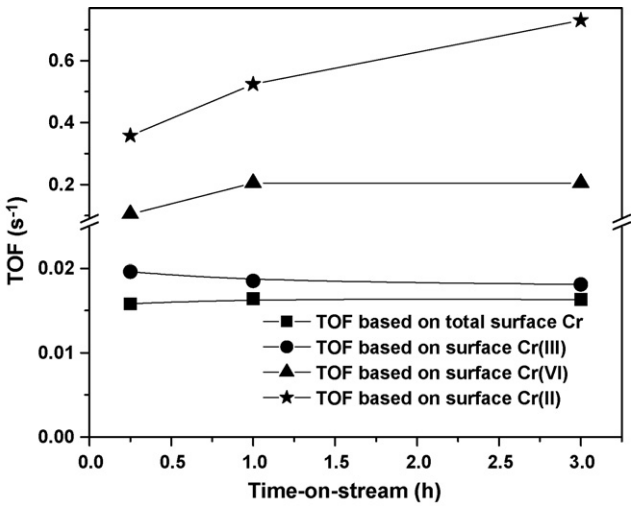

Fig. 9. TOF data for the 5Cr/PE-MCM-41 catalyst; temperature = 650 °C and $x_{C_2H_6}$ = 0.5.

concentration decreased with TOS due to the coke formation on the catalyst, but the relative concentration of various Cr species changed with TOS. As seen in Fig. 9, the TOF based on total surface Cr was relatively constant with TOS and this trend was similar to the TOF data considering Cr(III) alone as the active sites. The TOF data based on the Cr(II) and Cr(VI) sites increased with TOS, which is an unrealistic trend. Thus, the TOF vs. TOS data provide strong evidence that Cr(III) species are the likely active sites for ethane DH reaction.

4. Conclusions

Chromium oxide catalysts supported on high surface area, pore-expanded MCM-41 silica were synthesized and investigated for ethane DH. Reaction studies showed that the ethane conversion strongly depend on the chromia loading and the catalyst preparation method. In particular, the *x*Cr/PE-MCM-41 catalysts showed excellent performance in ethane DH in terms of activity, selectivity and stability. Correlation of quasi *in situ* XPS and UV–vis data with reaction rates provided strong evidence that Cr(III) species are the main active sites for the ethane DH reaction. Both Cr(VI) and Cr(II) species did not seem to play any significant role in the reaction.

Acknowledgements

A.S. thanks the Canadian Government for a Canada Research Chair in Catalysis by Nanostructured Materials (2001–2008). The generous support of the Natural Sciences and Engineering Research Council of Canada (NSERC) is acknowledged. Thanks to Mr. M.R. Pynenburg and Mr. R. Serna-Guerrero for their assistance with the synthesis of large-pore MCM-41 material and the TGA experiments, respectively.

References

[1] B.M. Weckhuysen, R.A. Schoonheydt, Catal. Today 51 (1999) 223.
[2] M.M. Bhasin, J.H. McCain, B.V. Vora, T. Imai, P.R. Pujado, Appl. Catal. A: Gen. 221 (2001) 397.
[3] D. Sanfilippo, I. Miracca, Catal. Today 111 (2006) 133.
[4] A.K. Rovik, A. Hagen, I. Schmidt, S. Dahl, I. Chorkendorff, C.H. Christensen, Catal. Lett. 109 (2006) 153.
[5] K. Nakagawa, M. Okamura, N. Ikenaga, T. Suzuki, T. Kobayashi, Chem. Commun. 9 (1998) 1025.
[6] F.M. Ashmawy, J. Chem. Soc., Faraday Trans. I 76 (1980) 2096.
[7] H.J. Lugo, J.H. Lunsford, J. Catal. 91 (1985) 155.
[8] H. Yang, L. Xu, D. Ji, Q. Wang, L. Lin, React. Kinet. Catal. Lett. 76 (2002) 151.
[9] A. Tsyganok, P.J.E. Harlick, A. Sayari, Catal. Commun. 8 (2007) 850.
[10] A. Tsyganok, R.G. Green, J.B. Giorgi, A. Sayari, Catal. Commun. 8 (2007) 2185.
[11] U. Olsbye, A. Virnovskaia, O. Prytz, S.J. Tinnemans, B.M. Weckhuysen, Catal. Lett. 103 (2005) 143.
[12] B.M. Weckhuysen, A. Bensalem, R.A. Schoonheydt, J. Chem. Soc., Faraday Trans. 94 (1998) 2011.
[13] S. De Rossi, G. Ferraris, S. Fremiotti, E. Garrone, G. Ghiotti, M.C. Campa, V. Indovina, J. Catal. 148 (1994) 36.
[14] F. Cavani, M. Koutyrev, F. Trifiro, A. Bartolini, D. Ghisletti, R. Iezzi, A. Santucci, G.D. Piero, J. Catal. 158 (1996) 236.
[15] A. Sayari, M. Kruk, M. Jaroniec, I.L. Moudrakovski, Adv. Mater. 10 (1998) 1376.
[16] A. Sayari, Angew. Chem., Int. Ed. 39 (2000) 2920.
[17] M. Kruk, M. Jaroniec, V. Antochshuk, A. Sayari, J. Phys. Chem. B 106 (2002) 10096.
[18] P.J.E. Harlick, A. Sayari, Ind. Eng. Chem. Res. 45 (2006) 3248.
[19] P.J.E. Harlick, A. Sayari, Ind. Eng. Chem. Res. 46 (2007) 446.
[20] R. Serna-Guerrero, A. Sayari, Environ. Sci. Technol. 41 (2007) 4761.
[21] K.-Z. Hossain, C.M. Monreal, A. Sayari, Colloid Surf. B: Biointerf. 62 (2008) 42.
[22] A. Sayari, S. Hamoudi, Y. Yang, Chem. Mater. 17 (2005) 212.
[23] D.D. Das, P.J.E. Harlick, A. Sayari, Catal. Commun. 8 (2007) 829.
[24] D.D. Das, A. Sayari, J. Catal. 246 (2007) 60.
[25] T.V.M. Rao, Y. Yang, A. Sayari, J. Mol. Catal. A: Chem 301 (2009) 152.
[26] R. Merryfield, M. McDaniel, G. Parks, J. Catal. 77 (1982) 348.
[27] B. Liu, Y. Fang, M. Terano, J. Mol. Catal. A: Chem. 219 (2004) 165.
[28] A.B. Gaspar, C.A.C. Perez, L.C. Dieguez, Appl. Surf. Sci. 252 (2005) 939.
[29] B.M. Weckhuysen, I.E. Wachs, R.A. Schoonheydt, Chem. Rev. 96 (1996) 3327.
[30] A.B. Gaspar, J.L.F. Brito, L.C. Dieguez, J. Mol. Catal. A: Chem. 203 (2003) 251.
[31] L. Liu, H. Li, Y. Zhang, Catal. Commun. 8 (2007) 565.
[32] A. Bruckner, Chem. Commun. 20 (2001) 2122.
[33] A. Bruckner, Phys. Chem. Chem. Phys. 5 (2003) 4461.
[34] T.A. Nijhuis, S.J. Tinnemans, T. Visser, B.M. Weckhuysen, Phys. Chem. Chem. Phys. 5 (2003) 4361.
[35] T.A. Nijhuis, S.J. Tinnemans, T. Visser, B.M. Weckhuysen, Chem. Eng. Sci. 59 (2004) 5487.
[36] J.P. O'Connell, J.M. Haile, Thermodynamics Fundamentals for Applications, Cambridge University Press, New York, 2005, p. 450.
[37] R.C. Reid, J.M. Prausnitz, B.E. Poling, The Properties of Gases and Liquids, 4th ed., McGraw-Hill, New York, NY, 1987.
[38] A. Hakuli, M.E. Harlin, L.B. Backman, A.O.I. Krause, J. Catal. 184 (1999) 349.